NASA/TM–20240001480

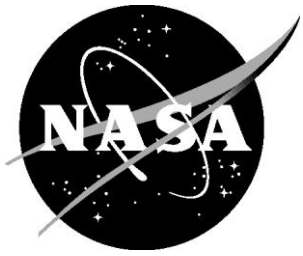

Mission and Vehicle-Level Updates for the Parallel Electric-Gas Architecture with Synergistic Utilization Scheme (PEGASUS) Concept Aircraft

Nathaniel J. Blaesser, Zachary J. Frederick, and Irian Ordaz
Langley Research Center, Hampton, Virginia

Felipe Valdez
Armstrong Flight Research Center, Edwards, California

Scott Jones
Glenn Research Center, Cleveland, Ohio

March 2024

NASA STI Program Report Series

Since its founding, NASA has been dedicated to the advancement of aeronautics and space science. The NASA scientific and technical information (STI) program plays a key part in helping NASA maintain this important role.

The NASA STI program operates under the auspices of the Agency Chief Information Officer. It collects, organizes, provides for archiving, and disseminates NASA's STI. The NASA STI program provides access to the NTRS Registered and its public interface, the NASA Technical Reports Server, thus providing one of the largest collections of aeronautical and space science STI in the world. Results are published in both non-NASA channels and by NASA in the NASA STI Report Series, which includes the following report types:

- TECHNICAL PUBLICATION. Reports of completed research or a major significant phase of research that present the results of NASA Programs and include extensive data or theoretical analysis. Includes compilations of significant scientific and technical data and information deemed to be of continuing reference value. NASA counterpart of peer-reviewed formal professional papers but has less stringent limitations on manuscript length and extent of graphic presentations.

- TECHNICAL MEMORANDUM. Scientific and technical findings that are preliminary or of specialized interest, e.g., quick release reports, working papers, and bibliographies that contain minimal annotation. Does not contain extensive analysis.

- CONTRACTOR REPORT. Scientific and technical findings by NASA-sponsored contractors and grantees.

- CONFERENCE PUBLICATION. Collected papers from scientific and technical conferences, symposia, seminars, or other meetings sponsored or co-sponsored by NASA.

- SPECIAL PUBLICATION. Scientific, technical, or historical information from NASA programs, projects, and missions, often concerned with subjects having substantial public interest.

- TECHNICAL TRANSLATION. English-language translations of foreign scientific and technical material pertinent to NASA's mission.

Specialized services also include organizing and publishing research results, distributing specialized research announcements and feeds, providing information desk and personal search support, and enabling data exchange services.

For more information about the NASA STI program, see the following:

- Access the NASA STI program home page at http://www.sti.nasa.gov

- Help desk contact information:

https://www.sti.nasa.gov/sti-contact-form/ and select the "General" help request type.

NASA/TM–20240001480

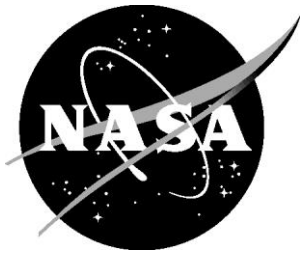

Mission and Vehicle-Level Updates for the Parallel Electric-Gas Architecture with Synergistic Utilization Scheme (PEGASUS) Concept Aircraft

Nathaniel J. Blaesser, Zachary J. Frederick, and Irian Ordaz
Langley Research Center, Hampton, Virginia

Felipe Valdez
Armstrong Flight Research Center, Edwards, California

Scott Jones
Glenn Research Center, Cleveland, Ohio

National Aeronautics and
Space Administration

Langley Research Center
Hampton, Virginia 23681-2199

March 2024

Acknowledgments

The authors thank Jesse Quinlan and Eric Hendricks for their guidance and input on the PEGASUS aircraft as well as Curt Hanson for his support of the dynamic stability and flying qualities modeling. The authors also thank Jason Kirk, Ty Marien, and Mark Guynn for editing and peer review. The NASA Advanced Air Transport Technology (AATT) project funded this research.

Available from:

NASA STI Program / Mail Stop 050
NASA Langley Research Center
Hampton, VA 23681-2199

Abstract

NASA created the PEGASUS concept with the goal of lowering mission energy (a surrogate for operating cost) compared to other regional aircraft by leveraging electrified aircraft propulsion (EAP). Since its inception, researchers have explored multiple facets of PEGASUS in varying fidelity but have not completed a rigorous, integrated design. The goal of this memorandum is to provide an updated design using recent studies and improved methods. This memorandum explores the initial vehicle concept and concept of operations, while considering ways to improve both the mission concept of operations and the integrated vehicle-level performance. Additionally, the design and analysis methodologies for EAP-enabled aircraft concepts are improved in several areas. This research incorporates new propulsion-airframe integration and wing weight surrogates to model the impacts of wingtip propulsors on the configuration. Detailed weight and balance calculations enable calculating dynamic stability and flying qualities within the conceptual design environment. Ultimately, the vehicle is optimized to reduce "well-to-wake" equivalent CO_2, CO_2e, rather than minimizing either fuel (or total energy) consumption or maximum takeoff weight. Using fuel/energy or takeoff weight leads to conflicting optima for hybrid-electric aircraft. Two aircraft are developed to provide points of comparison for PEGASUS: an advanced conventional turboprop vehicle and a hybrid-electric variant. The results show that the PEGASUS concept can reduce CO_2e relative to the advanced turboprop or a hybrid-electric propulsion architecture, albeit with an increase in maximum takeoff weight. PEGASUS's maximum takeoff weight is 55% heavier than the advanced conventional turboprop but it contributes 18% less CO_2e for a 400 nmi mission. For the same mission, PEGASUS's maximum takeoff weight is 47% heavier than the comparator hybrid-electric vehicle but it contributes 12% less CO_2e. This study shows that the PEGASUS configuration reduces CO_2e through its use of wingtip propulsors and that its benefit is not solely a result of switching to a hybrid-electric propulsion architecture. PEGASUS achieves this reduction in CO_2e while maintaining satisfactory Level 1 or 2 flying qualities for all of its longitudinal- and lateral-directional modes.

Nomenclature

C_L	=	Lift coefficient
C_D	=	Drag coefficient
C_x	=	Force coefficient in freestream direction
C_z	=	Force coefficient opposite of gravity
D	=	Propeller diameter
$\boldsymbol{D}$	=	Design variable vector for optimization
$\mathcal{F}$	=	Optimization objective function
F_x	=	Force in the freestream (x) direction
L/D	=	Lift-to-drag ratio
n_{prop}	=	Number of propulsors
n_z/α	=	Steady-state normal acceleration per unit change in angle of attack
P_{shaft}	=	Shaft power
q	=	Dynamic pressure
R_{tip}	=	Propeller radius
S	=	Wing reference area
t_w	=	Propeller twist distribution
T_2	=	Phugoid time to double amplitude
T_{2s}	=	Spiral time to double amplitude
V_V	=	Vertical tail volume coefficient
x	=	Flow direction (horizontal)
y^+	=	Non-dimensional initial grid height of CFD mesh
z	=	Direction opposite of gravity (vertical)
α	=	Angle of attack
ζ_p	=	Phugoid damping ratio
η_p	=	Propeller efficiency
θ	=	Radial distribution of blade pitch angle, $\theta = \theta_0 + t_w$
θ_0	=	Propeller collective (pitch) angle
θ_1	=	Tail strike angle of the aircraft
θ_2	=	Angle between the center of gravity, main landing gear, and vertical
λ	=	Propeller tip speed ratio
λ_p	=	Unstable phugoid root
τ_r	=	Roll mode maximum time constant
ω_{sp}	=	Short period natural frequency

1. Introduction

For the past seven years, the Parallel Electric-Gas Architecture with Synergistic Utilization Scheme (PEGASUS) concept has been a focus of NASA's Advanced Aircraft Transport Technology (AATT) portfolio. The genesis of the vehicle was Antcliff et al.'s research into regional air mobility and the potential impact that electrification can have on vehicle performance [1]. Ancliff's 2016 paper noted that many regional aviation trips could be served by a vehicle with a range of 400 nmi and that at this range, electrification could yield integrated performance benefits.

Antcliff and Capristan followed up the 2016 paper with the debut of the PEGASUS concept in their 2017 paper [2]. Figure 1a shows a rendering of the PEGASUS concept based on the 2017 paper. Based on the ATR 42-500, PEGASUS is a 40-passenger aircraft with a parallel hybrid-electric propulsion system featuring three propulsor classes. Figure 1b shows the original PEGASUS propulsors and their power sources. Hybrid-electric wingtip propulsors are sized for cruise and provide most of the cruise thrust. The electric inboard motors are used during takeoff and landing operations and conformally fold during cruise. The electric, aft boundary layer ingestion (BLI) propulsor operates during all phases of flight.

(a) Artist's rendering

(b) Propulsion system

Figure 1: The original PEGASUS concept rendering and propulsion system power sources.

PEGASUS is an example of a "technology collector" because it borrowed multiple features from the broad NASA aeronautics research portfolio and applied them to a regional aircraft. NASA's research into electrified aircraft propulsion (EAP) led to new aircraft configurations because the specific power of electric motors is higher and more scale-independent than that of gas turbine engines, which allows propulsors to be placed in unconventional locations on the airframe with the potential for aerodynamic benefits. For example, the original PEGASUS vehicle featured a BLI propulsor based on research from smaller EAP vehicles and the promising results of the Single-aisle Turbo-electric AiRCraft with an Aft Boundary Layer propulsor (STARC-ABL) concept [3–5][1]. Another EAP concept that influenced PEGASUS was the X-57 Maxwell, which features wingtip propulsors [7]. PEGASUS lessens the yawing moment generated from a critical loss of thrust (CLoT) by employing inboard propulsors that generate much of the takeoff thrust. Adopting another X-57 technology, the inboard propellers conformally fold to their nacelles during cruise to preserve a clean-wing lift distribution.

The original concept of operations (ConOps) calls for two potential missions: a 200 nmi, electric-only mission and a 400 nmi mission in a hybrid mode that uses both electricity and fuel

[1]This memorandum cites the original STARC-ABL paper because of its influence on BLI research. An updated memorandum, Ref. [6], corrects some of the initial work of Ref. [5] and shows more modest benefits of BLI propulsors.

to power the wingtip propulsors. The goal of the 200 nmi mission is to provide operators with an option for zero en route emissions during short-range missions. The ConOps poses challenges because the reserve mission requires an 87 nmi diversion to an alternate airport with an additional 45 minute loiter at 284 kts. The reserve mission thus has an equivalent distance of 300 nmi, which is longer than the all-electric mission cruise distance.

The goal of this research is to provide an updated design baseline for the PEGASUS concept, building on the past research and integrating all of the lessons learned. For clarity, the updated baseline is referred to as "PEGASUS 2.0" in this memorandum. Section 2 discusses past development efforts to create processes to analyze different facets of PEGASUS and their impact on the current aircraft. Section 3 describes the current research on the vehicle, as well as how it integrates with the past research to create a cohesive, closed design. Section 4 describes how the team developed the two comparison aircraft, an advanced conventional baseline (ACB) and a hybrid-electric baseline (HEB). Section 5 presents the results and final configuration for PEGASUS 2.0, including geometry details and mission performance. Sections 6 and 7 conclude the memorandum by summarizing the work and describing future research opportunities.

2. Past Studies

Since the initial PEGASUS concept paper in 2017, researchers at NASA and Georgia Tech have conducted several studies on individual facets of PEGASUS. Blaesser performed the first detailed aerodynamic study in 2019, investigating the induced drag benefit of wingtip propellers when compared with conventional, inboard-mounted propellers [8]. Though wingtip propellers were able to reduce the induced drag compared to inboard propellers, the lowest power consumption resulted from using all four wing-mounted propellers during cruise. The reason for this is that using four propellers decreases the thrust loading on each propeller, increasing each propeller's efficiency.

Later in 2019, Capristan and Blaesser created PEGASUS 1.0 [9] using the Layered and Extensible Aircraft Performance System (LEAPS) [10]. This research optimized the thrust split across the three propulsor classes during each mission phase and determined the total energy and fuel consumption as the ratio of electric motor power to gas turbine power of the wingtip propulsors varied. The ConOps still specified that the inboard propellers would fold during cruise. To account for increases in weight due to batteries, thrust-to-weight and wing loading ratios were held constant at the values for the conventional baseline. The principal result from that study was that approximately 80% of the shaft power supplied to the wingtip propulsors should come from the gas turbine engine in order to balance the increased battery weight needed for electric motor operation with fuel consumption.

Ordaz led an effort in 2020 [11] to develop an adjoint-based design capability within FUN3D [12] to minimize the power required by a propeller and applied this to the PEGASUS configuration. The capability allows efficient gradient-based optimization of propeller parameters, including diameter, tip speed ratio, twist and chord distribution, position, and orientation to minimize the shaft power required or maximize propeller efficiency to satisfy performance requirement constraints.

The wingtip propellers provide aerodynamic benefits but present challenges at the aircraft level. A failure of a wingtip propulsor will result in a large yawing moment that is difficult to correct, especially during low speed operations. In 2020, Blaesser and Frederick investigated various power architectures for CLoT scenarios during takeoff and found that applying a certain thrust distribution at takeoff can reduce the vertical tail size, though both the inboard and wingtip propulsors must be capable of independently generating most of the required takeoff power [13]. The paper assumed

that the specific volume of the hybrid wingtip propulsor and inboard motor would be similar, leading to large propulsors and an increase in wetted area compared to a conventional baseline. In retrospect, this was a poor assumption as electric motors have much higher power per unit volume and the inboard motors would likely be smaller, potentially resulting in a lower drag for PEGASUS than a conventional baseline.

Placing a large mass in the form of a propulsor at the wingtip has negative structural and aeroelastic impacts. Solano et al. at Georgia Tech performed a study on the wingtip propulsors' structural implications in 2021 [14]. The results provided NASA researchers with surrogate models to understand how different combinations of propulsor weights (wingtip and inboard) and wing geometry would impact the overall vehicle weight. A key insight from the Georgia Tech research is that considering static loads alone is insufficient for wingtip propulsors. Static loads from a wingtip propulsor alleviate the bending moment at the root and lead to a lower wing weight, but dynamic aeroelastic loads serve to offset this benefit by increasing the required wing weight.

In 2021, Frederick et al. performed a study on the impacts of aircraft layout and sizing on center of gravity (cg) location and flying qualities [15]. The study developed a process that distributes the weight, as predicted by the LEAPS weight analysis [16],[2] to the appropriate components within OpenVSP [18]. The process then uses OpenVSP's Mass Properties Toolbox to compute the cg and moments of inertia for the vehicle. Selected components, such as the battery, wing, and landing gear, are allowed to move within constrained limits to satisfy requirements such as tail strike angle, weight distribution on the landing gear, and static margin. VSPAero calculates the aircraft's stability and control derivatives to generate data for a six degrees of freedom (6DOF) simulator to check the vehicle dynamic stability and estimate its flying qualities. The framework provides for closed-loop component placement and vehicle dynamics.

3. Analysis Approach

As described in the previous section, PEGASUS has been the subject of numerous studies, but they have each focused on a single discipline and explored the trade space within that discipline. The current analysis effort is to integrate these results into a new vehicle design. Like PEGASUS 1.0, PEGASUS 2.0 maintains a constant thrust-to-weight ratio of 0.435 and wing loading of 70.0 lb/ft^2 to ensure that low speed performance is maintained. For sizing the battery, PEGASUS used a specific energy of 500 Wh/kg, a battery density of 2 kg/L, and a maximum depth of discharge of 80%. The general shape of the wing planform and the wing aspect ratio remain constant as wing area is varied. PEGASUS 2.0 incorporates research in integrated propeller-propulsor modeling, propulsion-airframe integration (PAI) surrogates, dynamic and static stability, wing weight surrogates, and integrated aircraft configuration design.

A. PEGASUS 2.0 ConOps

The ConOps for PEGASUS has changed from the original PEGASUS mission via eliminating the 200 nmi all-electric mission and all-electric reserve mission. The original 400 nmi mission remains and is the design mission for PEGASUS 2.0. Figure 2 shows the design mission profile, including the reserve mission.

The reason for removing the all-electric mission is primarily for operational considerations, though the all-electric reserve mission described earlier also presented sizing challenges. The wingtip propulsors are a parallel hybrid-electric architecture, which means that both the electric

[2]LEAPS and the Flight Optimization System (FLOPS) [17] use the same weight equations, thus Ref. [16] is appropriate

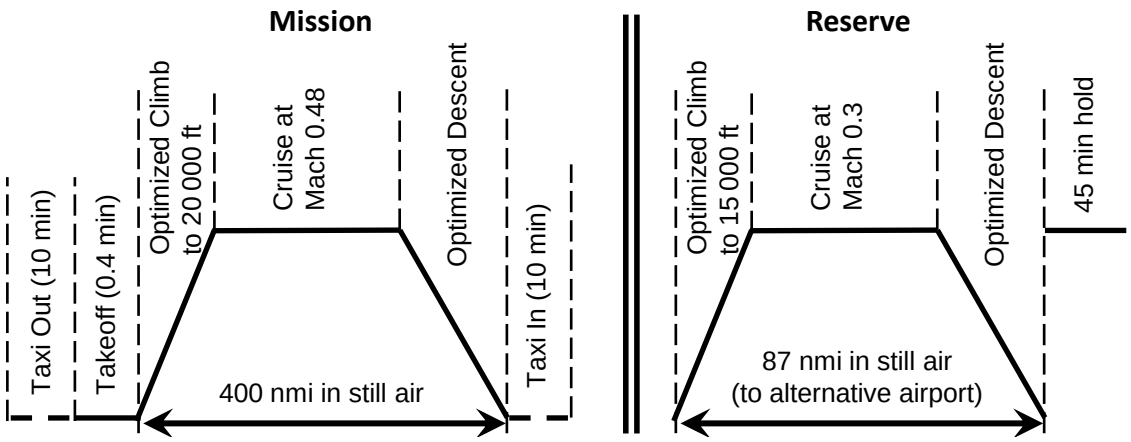

Figure 2: PEGASUS's design mission profile.

motor and the turbine cycle contribute power to the shaft. Removing one source of power requires a clutch mechanism, otherwise the inactive power source will remove productive work from the system. For example, if the turbine is inactive but still attached to the drive shaft, the electric motor will turn the compressor and turbines in addition to the propeller. Similarly, under normal operation, the turbine captures air through an inlet. If the turbine engine is not operated on a flight, i.e., during an all-electric mission, the inlet will produce ram drag unless the inlet is closed, further decreasing the vehicle's performance. Adding clutch mechanisms and covers for the turbine would ameliorate some of these drawbacks but at the expense of increased weight and complexity.

B. Aerodynamic and Aero-Propulsive Optimization via Surrogate Modeling

This research leverages the aero-propulsive predictions and adjoint-based design capabilities [11, 19] recently implemented in FUN3D 13.7 [12, 20], which includes the calculation of new functionals for shaft power, propeller efficiency, and net force along the x- and z-directions. FUN3D is a mixed-element, unstructured grid, Reynolds-Averaged Navier-Stokes (RANS) solver with a range of turbulence models and advanced features. The code has been developed by NASA and remains under active development. In FUN3D, the propellers are modeled as actuator disks with specified thrust and torque distributions along the blade span using blade element theory. This approach provides more refined control over the propeller design relative to uniformly loaded actuator disk models, as well as a way to calculate and model the torque imparted on the flow that produces swirl.

Two propulsor configurations are used to model the aero-propulsive effects. Figure 3a shows a conventional mid-span propulsor configuration used as a reference concept to quantify the aero-propulsive benefit associated with the PEGASUS configuration, shown in Fig. 3b, at a steady level flight cruise condition. The cruise condition was specified as a Mach number of 0.5, 20 000 ft altitude, and a 35 000 lb vehicle weight.

Surrogate Modeling Approach

Surrogate aero-propulsive models based on computational fluid dynamics (CFD) were developed to quantify the performance impact of the distributed propulsors on the PEGASUS concept. Surrogate models, which are fast in execution, are used in place of RANS CFD to predict aerodynamic performance and capture the aero-propulsive interactions between the airframe and

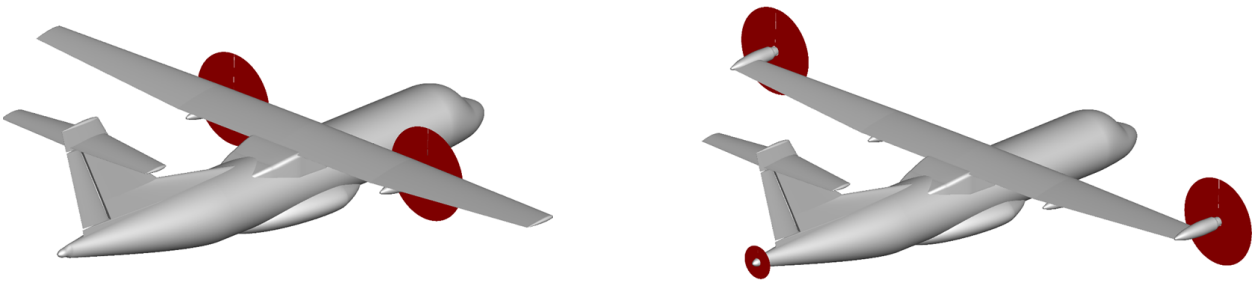

(a) Conventional reference. (b) PEGASUS (cruise).

Figure 3: Aero-propulsive configurations used to generate the surrogate models.

propulsors located at the wingtip and aft fuselage. This approach supports the integration of aero-propulsive optimization into a conceptual design and system level analysis of advanced concepts because it removes the heavy computational work required for CFD analysis.

The surrogate models were based on Gaussian process regression (GPR) and were developed using Scikit-Learn [21], a Python module for machine learning built on top of SciPy [22]. A full factorial design of experiments (DOE) was used to sample the domain and train the GPR model. The propulsor parametric space was decomposed into wingtip and BLI domains by assuming that the sensitivity of the aerodynamic performance with respect to each propulsor was independent, i.e., orthogonal, of one another. As a result, each propulsor had its own DOE consisting of 625 sample cases (four factors and five levels). This decomposition made the sampling of the design space more manageable by reducing the total number of CFD cases required to accurately capture the physics of the problem.

The full parametric space consisted of six propulsor design variables in addition to angle of attack, α. Three variables were used for each propulsor (wingtip and BLI propulsors): the tip speed ratio, λ, the actuator tip radius, R_{tip} (or diameter, D), and collective pitch control angle, θ_0. During parametric variations, the blade geometry (pitch angle and chord distribution) was held fixed to distributions that were optimized for minimum shaft power at the PEGASUS cruise condition. A Clark-Y airfoil was used to define the aerodynamic performance within the blade element theory actuator disks. A statistical analysis based on 649 random samples using a Latin hypercube (data that was not used to train the surrogate model) was used to verify the accuracy of the surrogate models. The maximum representation error for the random samples, when evaluated using the surrogate models, is less than 3% for the wingtip shaft power and less than 0.5% for both lift and drag coefficient, C_L and C_D.

CFD Analysis

The surrogate models were trained with aero-propulsive data calculated with FUN3D RANS for each DOE case described earlier. This aero-propulsive data includes aerodynamic force coefficients, C_L and C_D, as well as net force along the x-direction, F_x. For each propeller, the training data included shaft power, P_{shaft}, and propeller efficiency, η_p. The FUN3D mixed element grid, shown in Fig. 4, consisted of 20.5 million cells and 5.4 million nodes. The grid was generated with Pointwise [23] and HeldenMesh [24] for a y^+ of 0.8 at Reynolds number of 1.97 million per foot. Additional grid refinement was specified at the location of the actuator disks to accommodate the maximum diameter of the actuator disks allowed in the DOE parameter space. The FUN3D analyses were conducted on 2496 cores of Intel Haswell processors, dual-socket 12-core E5-2680v3 chip model with a base clock speed of 2.5 GHz. Each FUN3D flow solution consisted of 2000

iterations to achieve a reduction of three orders of magnitude in the density residual.

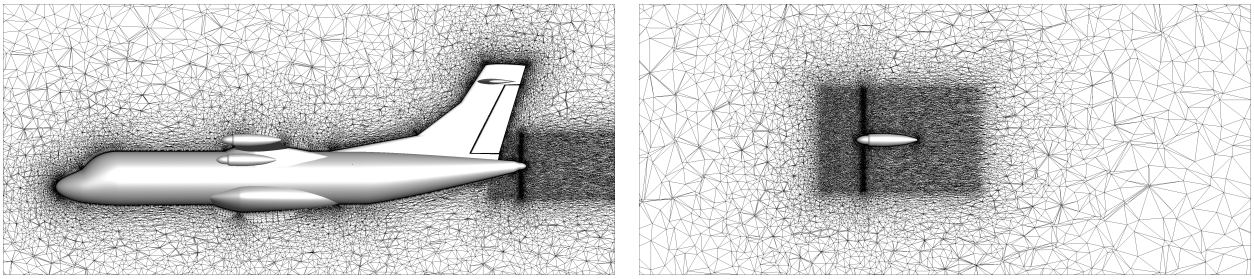

(a) Grid along aircraft centerline.

(b) Grid along the centerline of wingtip propulsor.

Figure 4: A visualization of the FUN3D mixed element grid.

The aero-propulsive benefit was quantified through the percent change in total drag of the PEGASUS concept relative to the reference concept (Fig. 3a). This reference concept was optimized with SNOPT 7.4-1.2 [25] and FUN3D to minimize the total shaft power at the cruise condition while satisfying the cruise performance constraint of zero net force on the vehicle. The total drag of the reference concept was then calculated using FUN3D through a sweep in angle of attack. For a given configuration of the wingtip and BLI propulsors (tip speed ratio, tip radius, and collective pitch control angle), the surrogate models were used to predict aerodynamic performance for a range of angles of attack. A numerical optimization routine was used to determine the angle of attack required for each C_L condition, and the percent change in total drag was calculated relative to the reference concept at a given C_L.

Aero-Propulsive Optimization and Evaluation of Surrogate Models

The aero-propulsive design characteristics were studied through the optimization of the PEGASUS concept at cruise using the surrogate models, with a verification of the final design through FUN3D analysis and optimization. The optimization problem is given in Eq. 1. Within Eq. 1, n_{prop} is the total number of propulsors and P_{shaft} is the shaft power of an individual propulsor. The C_x and C_z force coefficients are calculated by normalizing the net force along each of these directions by qS, where q is the dynamic pressure of 170 lb/ft^2 and S is the reference area of 596 ft^2. A negative value of C_x corresponds to a condition of excess thrust, a positive value of C_z corresponds to a condition of excess lift. The design variable vector, $\boldsymbol{D}$, included the angle of attack of the aircraft, α, tip speed ratio, λ, propeller tip radius, R_{tip}, and collective pitch angle, θ_0, for both the wingtip and BLI propulsors. The radial distribution of blade pitch angles along the blade, θ is the sum of the root pitch, θ_0 and twist distribution, t_w such that $\theta = \theta_0 + t_w$. The pitch distribution was the same across all propellers, implying the propeller blade had the same twist distribution and was operated at the same pitch setting. Lastly, design variables for the wingtip propellers were linked to ensure symmetric flight while maintaining opposite wingtip propeller rotation (inboard up).

$$\begin{aligned} &\text{Find: } \min_{\boldsymbol{D}} \mathcal{F} = 10 \sum_{i=1}^{n_{\text{prop}}} P^2_{\text{shaft},i} \\ &\text{Subject to:} \\ &\qquad C_x \leq 0 \\ &\qquad C_z \geq 0 \end{aligned} \tag{1}$$

Table 1 shows a comparison of the optimized PEGASUS concept using both the aero-propulsive surrogate models and the FUN3D adjoint-based design. The percent differences indicate an excellent agreement between the two optimization methods. The one exception is the excess thrust value, which is near zero for the surrogate yet 5.94 lb when calculated using FUN3D. Though this represented a nearly 100% difference, the total thrust generated by the vehicle is approximately 1300 lb. Thus, a six pound difference is actually quite small. For the excess thrust, some of the difference between the surrogate and the FUN3D value can be attributed to the difficulty in converging FUN3D, whereas a surrogate model can match equality constraints much more precisely.

Table 1: Comparison of Optimized PEGASUS Propulsor Design at Cruise

Parameter	Propulsor	Surrogate	FUN3D	Unit	% Difference
α	—	1.01	1.0	deg	1
C_L	—	0.349	0.347		0.58
C_D	—	0.0257	0.0257		0
F_x	—	0.0019	5.94	lb	99.7
P_{shaft} (total)	—	2600	2593	hp	0.24
λ	Wingtip	1.0	1.0		0
R_{tip}	Wingtip	5.91	5.93	ft	-0.34
θ_0	Wingtip	7.5	7.36	deg	1.9
P_{shaft}	Wingtip	1253	1243	hp	0.84
η_p	Wingtip	0.943	0.944		-0.1
Thrust	Wingtip	1224	1216	lb	0.62
λ	BLI	1.0	1.0		0
R_{tip}	BLI	2.0	2.14	ft	-6.5
θ_0	BLI	2.5	2.5	deg	0
P_{shaft}	BLI	93.1	107.8	hp	-13.6
η_p	BLI	0.927	0.931		-0.43
Thrust	BLI	111.4	130.4	lb	-14.6

Another important observation from Table 1 is that both optimization methods strongly favor the use of the wingtip propulsor over the BLI propulsor at the cruise condition. In fact, all BLI propulsor design variables (λ, R_{tip}, and θ_0) are driven to their respective lower bounds. In essence, the optimizer is attempting to eliminate the BLI propulsor. Although the BLI propulsor has a lower thrust-specific power requirement, it also produces a variation in pressure upstream on the aft region of the fuselage that results in an increase in fuselage drag. This is not unexpected, as previous work [19, 26] has shown that the optimization of a BLI system may require tailoring of the geometry upstream of the propulsor. However, parameterization of the upstream geometry was not considered in this study because it would significantly increase the number of design variables that would need to be included in the DOE used to train the surrogate models. This would make the calculation of the training data with FUN3D significantly more computationally expensive.

Figure 5 shows the variation of aero-propulsive benefit as a function of C_L for the optimized PEGASUS configuration from Table 1. The reduction in total drag is relatively linear up to a C_L of approximately 0.42, where it reaches a value of -11.4%. Because the optimizer sought to minimize the use of the BLI propulsor for the PEGASUS configuration, the team chose to remove it from this PEGASUS 2.0 configuration.

The surrogate models were evaluated to determine if they could be used in place of FUN3D

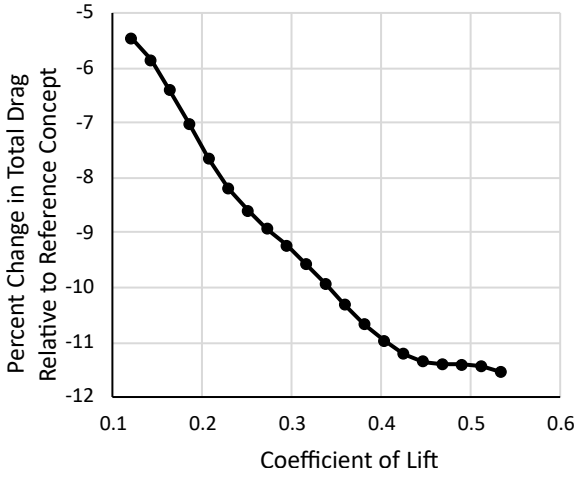

Figure 5: Aerodynamic benefit of the PEGASUS configuration.

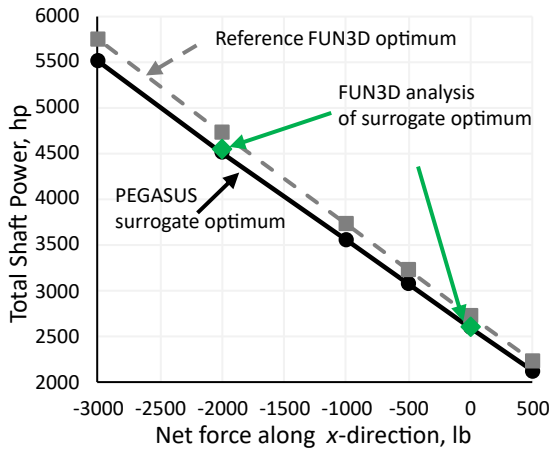

Figure 6: Verification of surrogate models for total shaft power.

within a conceptual design process. Figure 6 shows a comparison of total shaft power at different net forces in the x-direction between PEGASUS and the conventional reference concept. For this analysis, the PEGASUS model only included wingtip propulsors, i.e., no BLI propulsor. The variations in net force were achieved through changing the propeller pitch and tip speed ratio to affect the thrust level on each vehicle. The dashed line denotes the total shaft power for both propulsors on the conventional reference concept at various thrust conditions. Similarly, the solid line denotes the total shaft power for both wingtip propulsors for the PEGASUS configuration optimized using the aero-propulsive surrogate models. The percent decrease in total shaft power for the PEGASUS configuration at cruise ($F_x = 0$) is 4.6%. As a verification, the optimized propulsor designs (including angle of attack) for $F_x = 0$ and $F_x = -2000$ lb were analyzed with FUN3D and their corresponding total shaft power is plotted with the scatter green point markers. The error in optimized total shaft power between the surrogate models and FUN3D is less than 1% for these two configurations.

C. Propulsion Modeling

Exploring the design space of the propulsion architecture requires gas turbine and electric motor data for various maximum power levels, combined with a propeller model to turn power into thrust. The gas turbines were simulated in the Numerical Propulsion System Simulation (NPSS) [27] and based on the Pratt & Whitney PW 127E turboprop. The modeled engines had maximum shaft powers ranging from 600 shaft horsepower (SHP) to 2400 SHP. Intermediate maximum power settings were created by interpolating between NPSS models. The wingtip and inboard motor powers varied from 100 kW to 1000 kW and 100 kw to 1200 kW, respectively.

Regardless of whether the power comes from an electric motor or a gas turbine engine, power must be turned into thrust via a propeller. For this study, XROTOR [28] was used to predict the propeller performance based on the propeller diameter and number of blades for the ATR 42-500, the vehicle on which PEGASUS was based. Using the same number of blades and diameter as the reference aircraft for all propulsors on PEGASUS was a simplifying assumption. In general, larger diameter propellers can have higher efficiencies, though the structural characteristics of the blades limit the diameter. This research did not conduct detailed propeller design to ensure

a different propeller geometry—twist and chord distributions withstanding—would meet all flight requirements. The velocity and density came from the top-of-climb operating conditions. Rather than specify an actual airfoil, the airfoil's design lift coefficient was varied until an optimal value was found for the cruise condition. This approach for propeller modeling was previously used by Marien et al. [29, 30].

The sizing of each individual propulsor's power requires clarification. The overarching takeoff thrust levels were set by the aircraft's maximum takeoff weight (MTOW) and desired thrust-to-weight ratio of 0.435. A series of propeller models were created in XROTOR for different design power levels. Each propeller model was then operated at each Mach, altitude, and power setting for the mission to create a library of engine decks with different sea-level static (SLS) thrust values. By requiring an SLS thrust target for a certain configuration, an appropriate engine deck could be interpolated from the engine deck library. The takeoff power setting was achieved by distributing the power between the inboard propulsor and wingtip propulsor, and the wingtip power was split between the gas turbine and the electric motor. Additionally, the gas turbine power setting at takeoff was allowed to vary so that only a fraction of the available power was used. Thus, there were three degrees of freedom for the propulsion system: the inboard motor power, the wingtip motor power, and the percentage of the gas turbine power used at takeoff. These three inputs resulted in two metrics that were used to track vehicle performance: the first was the ratio of wingtip-to-inboard thrust at takeoff, and the second was the overall hybridization of the aircraft. The takeoff thrust distribution and overall hybridization metrics were more intuitive to track compared to the three input values. Because these two metrics were results of the simulation, they could not be directly input into the model.

D. Center of Gravity Placement, Static Stability, and Geometric Constraints

Frederick et al. established a means of estimating the cg placement for PEGASUS to ensure the concept was longitudinally statically stable [15]. Additionally, this process ensured that constraints based on the aircraft's geometry, such as tail strike angle, were satisfied. The process was the result of integrating a mass properties model in OpenVSP and a mission analysis model in LEAPS. Incorporating LEAPS allowed weight and balance impacts to PEGASUS to be evaluated in terms of figures of merit such as block fuel or energy. Parameters of interest included electric motor size, battery placement, and wing placement.

Static margin was held constant when performing design trades to ensure that different configurations had similar longitudinal stability characteristics. The Mass Properties Toolbox within OpenVSP enabled the estimation of cg location for each configuration. A semi-empirical method by Caughey [31] was used for estimating neutral point. To hold static margin fixed, the horizontal tail area was scaled to position the neutral point for a given cg location. This low fidelity method of evaluating aircraft stability facilitated rapid trades through the design space; however, it did not consider lateral and directional stability or the dynamic response of the vehicle. This method was used to identify promising configurations that were then evaluated using a higher fidelity 6DOF model to confirm the stability characteristics were satisfactory.

When aircraft utilize batteries as a part of the propulsion system, the battery location is a major driver of the cg location. In addition to cg concerns, there are also volumetric constraints to physically placing large batteries within the outer mold line (OML). To address this, the method took the calculated battery weight from LEAPS, computed the battery volume based on a density of 2 kg/L, and attempted to place the batteries within the underfloor compartment of the fuselage and within the wing. If the required battery volume was larger than the volume available, the case was discarded.

The team used the requirements for static margin; tail strike angle; and the angle created by the cg, the main landing gear, and vertical axis. Figure 7 shows the tail strike angle as θ_1 and the angle between the main landing gear, cg, and vertical as θ_2. The target for a nominal static margin was 10%; for θ_1 and θ_2 the target was 15°. The angle between the main landing gear and cg is a surrogate for ground loading stability and the vehicle's ability to rotate during takeoff. If the angle is too small, the aircraft is susceptible to tip-over during certain loading operations. If the angle is too large, the vehicle will have trouble rotating during takeoff.

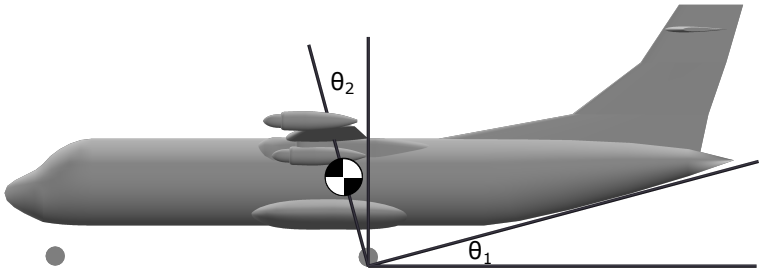

Figure 7: Depiction of the constrained angles for weight and balance estimation.

E. Dynamic Stability and Flying Qualities

Aircraft linear models and a 6DOF time-based simulation were developed to evaluate the impacts of design choices on the dynamic stability and flying qualities of the PEGASUS aircraft. Mass properties, aerodynamics, and propulsion models from the conceptual design tools were integrated using MathWorks SIMULINK simulation software [32]. The PEGASUS dynamic stability analysis was a two-step process. Step 1 used a nonlinear simulation to trim the aircraft at a specified flight condition and output linear models for flying qualities analysis and autopilot design. Step 2 incorporated the autopilot and evaluated specific cases such as setting the pitch attitude to achieve the desired climb rate and reach a commanded altitude. Dynamic stability results were analyzed and used to provide updates to the configuration in LEAPS. The next section describes this integrated design process in detail.

F. Code Integration Efforts

LEAPS was the integrator for all the previous analyses because of its ability to perform mission analysis for hybrid-electric vehicles, and OpenVSP was the geometry modeler for the vehicle. These two tools formed the center of the workflow and were able to receive and distribute key aircraft parameters such as geometric information, component weights, control surface sizes, and more. For example, CLoT requirements sized the empennage and the dimensions were passed to OpenVSP. The OpenVSP model, with updated empennage sizing, was passed to the dynamics and control module for building the 6DOF nonlinear simulation.

The aero-propulsive surrogates were used to quantify the PAI effects of wingtip propulsors relative to an inboard configuration. The LEAPS aerodynamic model was calibrated such that its drag polar for the baseline vehicle matched the drag polar produced by the surrogates. The surrogates computed the difference in total drag between the wingtip configuration and the inboard configuration across a range of C_L. This information was used to create a single lookup table of drag benefits as a function of C_L. This lookup table was held fixed and used for all configurations. The drag benefit was bookkept as a drag reduction term that was added to the total drag of the

vehicle at cruise. The code then iteratively ran the LEAPS mission analysis, updated the assumed C_L with the actual C_L of the vehicle at cruise and recalculated the drag benefit, until C_L converged.

Figure 8 shows an example of the workflow, LEAPS calculated the vehicle's component weights and passed them to the cg and static margin calculating code. An exception to this was the wing weight, which was based on the surrogate models developed by Solano et al. [14] and used to override the weight calculated by LEAPS. The cg and static margin results were then fed into the dynamics and control model to determine if the vehicle was dynamically stable and had acceptable handling qualities. LEAPS was then used to perform mission analysis to assess the fuel and electric energy consumed during the mission. Ultimately, this information was translated into a "well-to-wake" equivalent CO_2 metric, CO_2e, wherein the global warming potentials for the various emissions associated with the production and use of the onboard energy (fuel and electricity) were converted to an equivalent amount of CO_2. For example, the impact of a pound of methane on global warming is approximately 25 times greater than a pound of CO_2, thus a pound of methane would have a CO_2e of 25 lb. The CO_2e emissions for the electricity used to charge the onboard battery assumed a future US electric power grid where coal powered power plants have been phased out and replaced with sustainable electricity generation [29]. The CO_2e metric was used as the objective function for determining the optimum configuration.

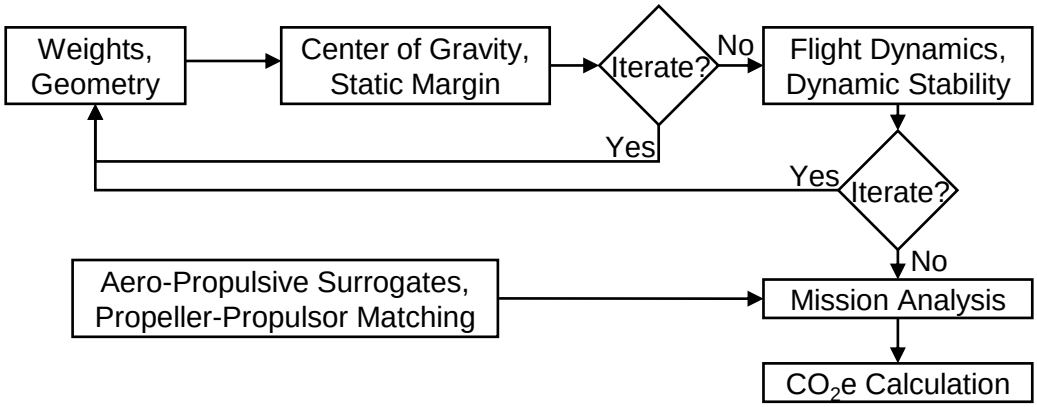

Figure 8: A notional flowchart depicting how the final PEGASUS codes were integrated.

4. Development of the Comparison Aircraft

Two additional aircraft were created in order to properly assess the PEGASUS concept and isolate the benefits inherent to the unique PEGASUS configuration from those of a more traditional configuration also employing a hybrid-electric propulsion system. The conventional vehicle is called the advanced conventional baseline (ACB) and the conventional vehicle with a hybrid-electric propulsion system is called the hybrid-electric baseline (HEB). Figure 9 is a top view diagram, showing the type and location of the propulsors on each vehicle.

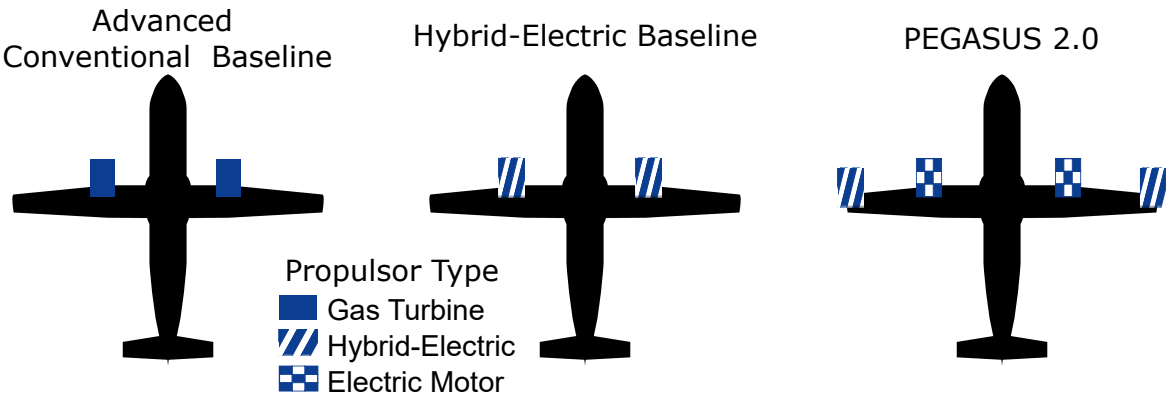

Figure 9: From left to right: ACB, HEB, and PEGASUS 2.0 configuration.

The ACB is an ATR 42-like aircraft featuring advanced technologies commensurate with an entry into service (EIS) of 2035. This vehicle features advanced composite materials to save weight, aerodynamic improvements to decrease drag, and modernized engines to decrease fuel consumption across the mission. The workflow placed the ACB's wing along the fuselage such that the cg was at the quarter chord. The HEB was sized using the same methodology as the ACB, and the longitudinal position of the batteries was adjusted to maintain the cg location and static margin. The HEB features parallel-hybrid propulsors in the traditional inboard location, as opposed to placing them at the wingtips, and the same technological updates as the ACB. To understand the impact of electric motor throttling on CO_2e, the electric motor throttle of the HEB was varied during sizing. The results show no benefit from operating the electric motor at partial powers, thus the electric motor was operated at full power for the entire mission. A sweep of electric motor powers was performed with a 100 kW electric motor showing the greatest CO_2e benefits for the HEB. The ACB and HEB were sized to fly the same design and reserve mission as PEGASUS, previously shown in Fig. 2. The vehicles were designed using the same process as PEGASUS to ensure consistency in approaches by maintaining constant thrust-to-weight, wing loading, and aspect ratio, and using the same wing weight surrogates. The CLoT vertical tail sizing and horizontal tail sizing based on desired static margin maintained a consistent empennage sizing approach.

The wing weight surrogates developed for PEGASUS do not extend to a weightless wingtip propulsor and therefore could not be applied to the ACB or HEB vehicles without additional data. To generate the requisite data, the same detailed analysis used to generate the wing weight surrogates was completed for a single data point with a weightless wingtip propulsor. The difference in wing weight between this analysis and the wing weight predicted by the surrogates was used to calculate a calibration factor to apply for a weightless wingtip propulsor.

5. Results and Discussion

A. Sizing Analysis and Mission Performance for PEGASUS 2.0

The design exploration varied three independent parameters—wingtip motor power, inboard motor power, and gas turbine (GT) throttle used at takeoff—which resulted in two output parameters, the thrust distribution between wingtip and inboard propulsors and the overall hybridization. Figure 10 shows contours of percent change in CO_2e with respect to the ACB, the figure of merit

used to select the final PEGASUS 2.0 configuration. This exploration revealed a large design space of feasible PEGASUS configurations with two regions of infeasible designs. First, the proportion of takeoff thrust generated by the inboard propulsor was limited by the fact that the wingtip propulsor needed to provide enough thrust at cruise to overcome drag. As the inboard motor power was increased, the wingtip propulsor had to be downsized to maintain the thrust-to-weight ratio until eventually the wingtip propulsor was no longer able to supply enough thrust at cruise. This is evident in Fig. 10 by the blank space representing infeasible solutions in the lower-left corner of each subfigure. Second, higher levels of hybridization led to heavier aircraft and required higher takeoff thrust to maintain thrust-to-weight ratio. At certain combinations of inboard and wingtip motor power, the engine power of the wingtip propulsor was greater than the largest GT in the engine library. Therefore, for high levels of hybridization, a greater share of thrust at takeoff had to be allocated to the inboard propulsors than was required for lower levels of hybridization. The infeasible region imposed by the maximum engine data set size is shown in Fig. 10 by the blank space in the upper-right corner of each subfigure.

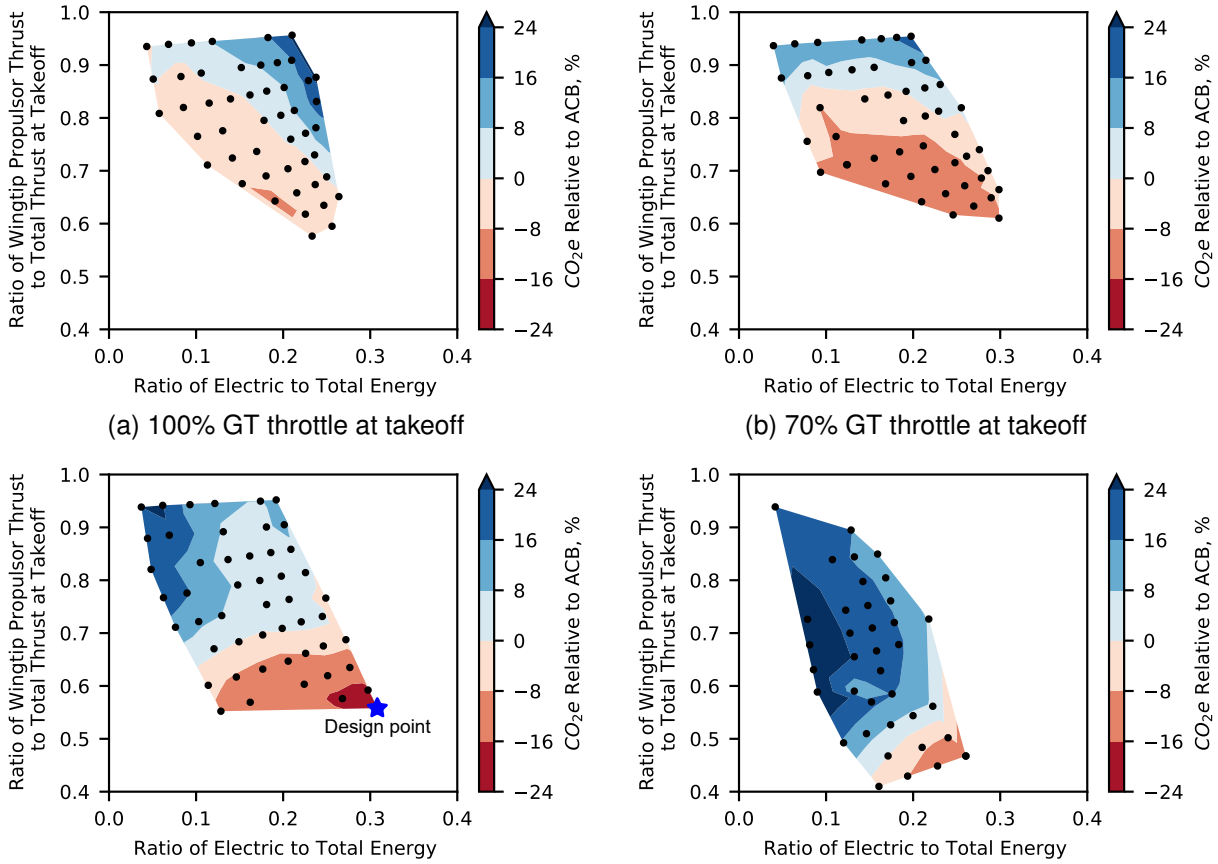

(a) 100% GT throttle at takeoff

(b) 70% GT throttle at takeoff

(c) 50% GT throttle at takeoff

(d) 30% GT throttle at takeoff

Figure 10: Contours of percent change in CO_2e relative to ACB for thrust split versus hybridization. PEGASUS 2.0 configuration which minimizes CO_2e is shown with a blue star.

Higher levels of hybridization were not prevented by volumetric constraints on the battery, with the most hybrid cases only using approximately 70% of the total volumetric capacity of the fuselage and wing. If an analysis case had resulted in a larger required battery than PEGASUS's

available internal volume, the case would have been removed from the feasible design space. Appendix A contains trades of other important parameters with respect to the ACB, including MTOW, vertical tail volume coefficient (V_V), and block fuel. None of these parameters directly factored into determining the design point, though PEGASUS 2.0 has the same design point for the minimum CO_2e and minimum fuel consumption, as shown in Appendix A.3.

Figure 11 highlights two vehicle-level trades using the 50% GT throttle at takeoff as a representative example. Figure 11a shows how MTOW quickly grew with increasing hybridization. The highest levels of hybridization studied resulted in weights that exceeded the library of gas turbine engine models and were therefore unfeasible. (Figure 11a also shows that optimizing on MTOW would have resulted in a different optimal configuration for PEGASUS.) Figure 11b shows how V_V was primarily influenced by the thrust split between the wingtip and inboard propulsor at takeoff, with V_V being nearly double the ACB value if all takeoff thrust comes from the wingtip propulsor. The consequence of losing a wingtip propulsor at takeoff, with its large yawing moment, would require a large vertical tail to comply with federal regulations relating to controllability during a CLoT.

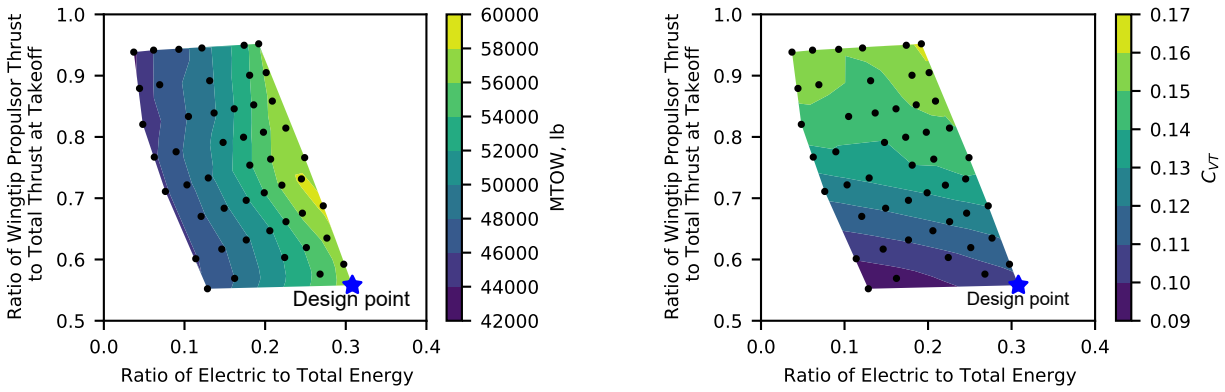

(a) Contours of MTOW in lb.

(b) Contours of vertical tail volume cofficient.

Figure 11: Contours of MTOW and vertical tail volume coefficient for 50% GT throttle at takeoff. The blue stars show the minimum CO_2e design.

Figure 12 shows a comparison of the CO_2e across the concepts. A key takeaway is that the PEGASUS configuration offers a 12% CO_2e benefit over a hybrid-electric baseline, showing that CO_2e benefits come from the wingtip propulsors and not just the hybrid-electric propulsion system. Compared to the ACB, PEGASUS reduces CO_2e emissions by 18%. The HEB shows a 7% reduction in CO_2e despite being a low level of hybridization. This CO_2e benefit is the result of the electric power grid being "cleaner" (having lower CO_2e emissions than a gas turbine engine) and the higher system efficiencies afforded to electric powertrains.

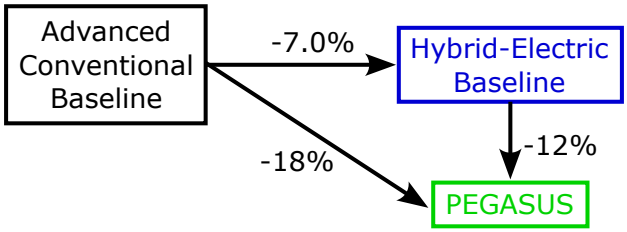

Figure 12: Percent change in CO_2e between configurations.

Figure 13 is an infographic that summarizes the three vehicles and their differences. The image on the left overlays the OMLs of the concepts to highlight their relative sizes. The ACB and HEB are nearly identical in terms of size and weight. PEGASUS 2.0 is much heavier, which results in a larger wing and empennage. The vertical tail is disproportionately large compared to a conventional aircraft of similar weight due to the wingtip propulsors. The ability to use battery weight to control the cg location enables PEGASUS 2.0 to maintain its cg, which meant the horizontal tail area did not need to be much greater than the comparators' horizontal tail areas. The resulting horizontal tail volume coefficient for PEGASUS 2.0 is much smaller than those of its comparator aircraft.

The table on the right of Fig. 13 provides geometry and weight information. The following PEGASUS 2.0 configuration minimizes the chosen figure of merit, CO_2e: 600 kW wingtip motor, 1000 kW inboard motor, 50% GT throttle at takeoff. This point is marked with a blue star on Figs. 10 and 11. For the HEB, CO_2e is minimized with a 100 kW electric motor. Of note, the 100 kW electric motor was the smallest electric motor size allowed during the HEB sizing process. A smaller electric motor may lead to a lower CO_2e total. Figure 14 shows a three-view diagram of the final PEGASUS 2.0 configuration and Table 2 summarizes the vehicle's performance data.

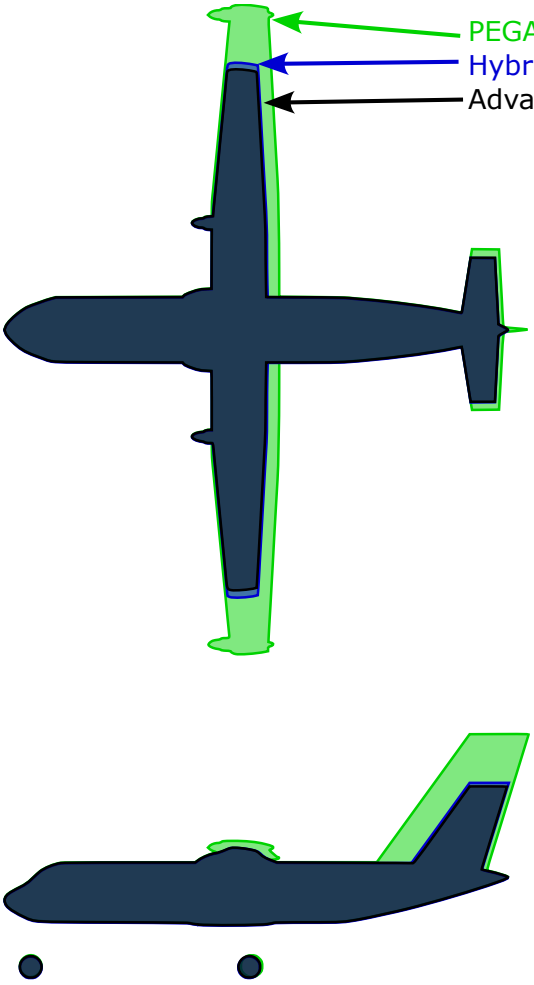

		ACB	HEB	PEGASUS 2.0
Wing	Span, ft	76.4	78.4	95.2
	Area, ft^2	527	555	818
Horizontal Tail	Area, ft^2	101	101	126
	Volume Coef.	0.976	0.882	0.623
Vertical Tail	Area, ft^2	110	120	274
	Volume Coef.	0.089	0.090	0.107
Propeller	Diameter, ft	6.45	6.45	6.45
Weights	MTOW, lb	36 850	38 860	57 270
	OEW, lb	23 400	24 040	30 700
	Fuel, lb	1450	1320	925
	Battery, lb	0	1456	13 600

Figure 13: Overlay of the ACB, HEB, and PEGASUS 2.0 with key geometric and weight data.

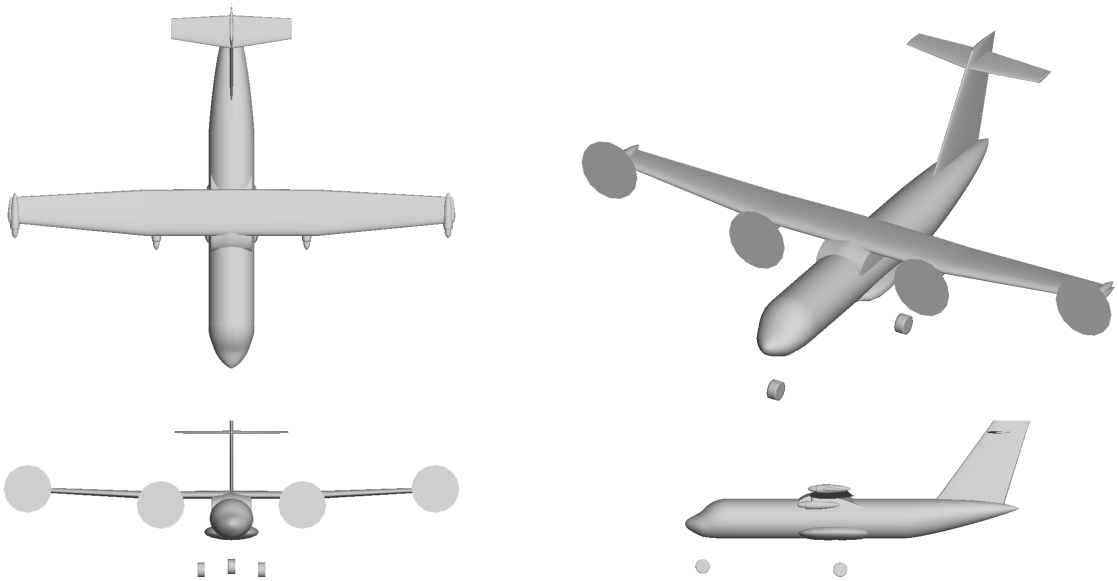

Figure 14: Multi-view renderings of PEGASUS 2.0.

Table 2: PEGASUS and Reference Configuration Performance Data

	Units	ACB	HEB	PEGASUS 2.0
Max power output of one GT at takeoff	hp	2380	2530	2090
Wingtip thrust (single propulsor, GT @ 50% throttle)	lb	–	–	6950
Inboard thrust (single propulsor)	lb	8020	8460	5510
Total takeoff thrust (all propulsors)	lb	16 040	16 920	24 920
Thrust at start of cruise	lb	2520	2610	3850
Electric power at start of cruise	kW	–	200	1570
Fuel consumption at start of cruise	lb/hr	1055	997	771
Thrust specific fuel consumption	lb/hr/lb	0.42	0.38	0.20
Thrust specific energy consumption	kW/lb	2.28	2.08	1.09
L/D at cruise	–	14.5	14.8	14.8
Total Energy	MJ	28 300	26 630	26 170
CO_2e	lb	5440	5060	4470

B. Dynamic Stability and Flying Qualities

Dynamic stability results for PEGASUS 2.0, the ACB, and HEB are presented here using criteria from MIL-STD-1797B [33] and MIL-8785C [34] for Category B (cruise flight) Class II transport airplanes. Ideally, a combination of both Federal Aviation Regulations (FAR) and military standards would be used; however, the military standards are broadly used for transport aircraft stability and control requirements and are suitable as an initial set of requirements. Longitudinal flying qualities are further described by the phugoid (long period) and short period modes. The phugoid mode is a lightly damped, low frequency oscillatory motion representing vertical translation related to a

tradeoff between kinetic and potential energy. The phugoid mode, characterized by its damping ratio, ζ_p, for all three configurations is very lightly damped but stable, making it marginally Level 2 as shown in Table 3. The addition of a pitch rate and attitude stability augmentation system could potentially increase the phugoid damping to provide Level 1 flying qualities [35]. Within Table 3, T_2 is the time to double in amplitude for the phugoid, defined in Eq. 2, where λ_p is the value of the unstable root.

$$T_2 = \frac{\ln(2)}{\lambda_p} \tag{2}$$

Table 3: Phugoid Damping Ratio Criteria (ζ_p) for Category B

MIL-F-8785C Criteria		ACB	HEB	PEGASUS 2.0
Level 1	$\zeta_p \geq 0.04$	—	—	—
Level 2	$\zeta_p \geq 0.00$	0.0254	0.0221	0.0253
Level 3	$T_2 \geq 55$ seconds	—	—	—

Figure 15 illustrates the pitch short period flying qualities with the red boxes denoting the boundaries of each flying quality level. The control anticipation parameter (CAP) in Fig. 15 was calculated from Eq. 3, where ω_{sp} is the short period natural frequency and n_z/α is steady-state normal acceleration per unit change in angle of attack.

$$CAP = \frac{\omega_{sp}^2}{n_z/\alpha} \tag{3}$$

The short period mode is a highly damped, high frequency oscillatory motion representing pitch rotations about the center of gravity. All three vehicle configurations are longitudinally stable and met short period mode Level 1 criteria, with PEGASUS 2.0 near the Level 2 boundary of the damping axis. Increasing the horizontal stabilizer and elevator area would provide a higher pitch damping for PEGASUS 2.0 at a cost of a heavier aircraft with more drag. The addition of a pitch damper would also provide an increase in pitch damping, which would move the PEGASUS 2.0 short period criteria further away from the Level 2 boundary. A pitch damper is an augmented control system that continuously monitors the vehicle's pitch rates and moves the elevator, via an elevator servo, to rapidly neutralize those pitch rates, providing improved damping for the short period characteristics.

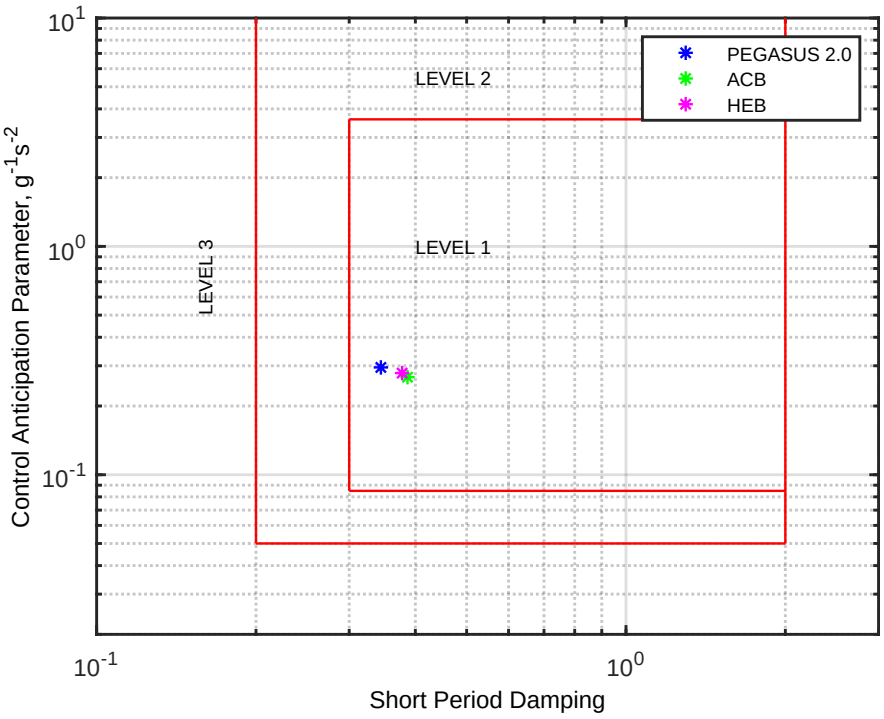

Figure 15: CAP versus short period damping criteria for Category B.

Lateral-directional flying qualities are described by the Dutch roll, spiral, and roll subsidence modes. Figure 16 shows that the Dutch roll mode for the ACB and HEB is marginally Level 2, and that the addition of a yaw damper would provide Level 1 flying qualities. A yaw damper is an augmented control system that continuously monitors the vehicle's yaw rates and moves the rudder, via a rudder servo, to rapidly neutralize yaw rates, providing more damping for the Dutch roll mode. The yaw damper prevents Dutch roll motion that, if not corrected, can become dynamically divergent and cause loss of control. However, careful consideration needs to be given to the bare airframe Dutch roll mode, as a malfunction of the yaw damper could cause severe oscillations leading to irrecoverable loss of control [36]. The Federal Aviation Administration (FAA) suggests that the yaw damper should be disabled for takeoff and landing since terminal flight phases are often the most safety critical for the mission and an active yaw damper creates another failure mechanism [37]. Figure 16 shows that PEGASUS 2.0 does not need a yaw damper to meet Level 1 criteria, which is a result of PEGASUS's larger vertical tail size. However, it was found that too large of a vertical stabilizer induces an unstable spiral mode, which results from excessive directional stability relative to lateral stability [38, 39].

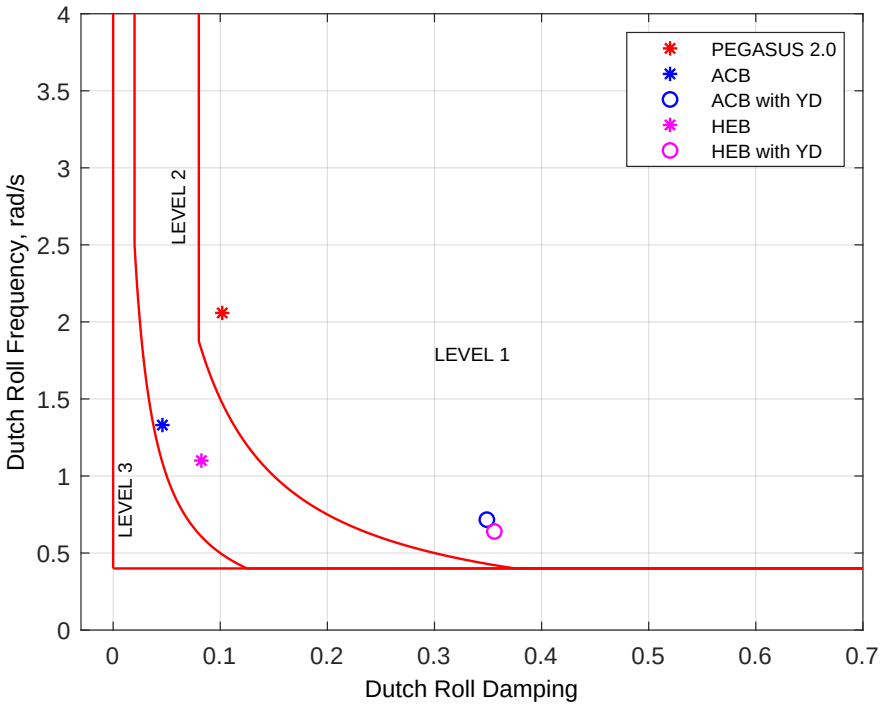

Figure 16: Dutch roll frequency versus damping criteria for Category B.

The spiral mode is characterized by slow rolling and yawing responses to a roll disturbance. During fully attended operations (takeoff, landings, etc.), spiral divergence is generally not a problem for the pilot. However, it can be a nuisance and even a safety issue during low-gain tasks (e.g., Instrument Landing System approach) if the divergence is too rapid. A limit on time to double bank angle amplitude for the spiral mode is necessary for safety during such operations. Table 4 outlines the maximum allowable time for spiral divergence during non-terminal flight phases. Because there are not specific requirements for spiral stability (convergence) for any aircraft, a converging spiral mode was deemed to meet MIL-F-8785C / MIL-STD-1797B Level 1 criteria. The ACB and HEB have a convergent spiral mode, therefore meeting Level 1 criteria. Conversely, PEGASUS 2.0 has a divergent spiral mode while also meeting Level 1 criteria. This spiral instability may be caused by insufficient fin surface above the cg coupled with either too much fin surface to the rear or a rudder control surface that is too large. [40]. Analysis showed that reducing the vertical tail size or increasing the dihedral angle in the outer section of the wing improved PEGASUS's natural spiral stability, making it stable. However, this reduced the Dutch roll damping, pushing the Dutch roll mode back to Level 2 flying qualities. Additionally, a stability augmented system having a sideslip angle feedback to aileron, providing a rolling moment due to sideslip, can improve the dihedral effect, which can help in stabilizing the spiral mode [41]. It is important to note that overcorrection of spiral instability may produce instability in the Dutch roll and vice versa. Given PEGASUS's Level 1 flying qualities with regard to the spiral mode, the vehicle does not need additional modifications from its initial design.

Table 4: Spiral Time to Double Criteria for Category B

MIL-STD-1797B Criteria		ACB	HEB	PEGASUS 2.0
Level 1	$T_{2s} > 12$ s	N/A	N/A	182 s
Level 2	$T_{2s} > 8$ s	—	—	—
Level 3	$T_{2s} > 4$ s	—	—	—

The last lateral-directional mode is the roll subsidence. This mode is a highly damped, non-oscillatory motion showing how rolling motion is damped. Table 5 shows the roll mode maximum time constants, τ_r, per MIL-STD-1797B criteria and time constants for the three different aircraft configurations. PEGASUS 2.0 has a higher time constant than the other two aircraft due to the much higher roll inertia induced by the wingtip propulsors. All vehicles meet Level 1 criteria indicating good roll control characteristics.

Table 5: Roll Subsidence Time Constant Criteria for Category B

MIL-STD-1797B Criteria		ACB	HEB	PEGASUS 2.0
Level 1	$\tau_r \leq 1.4$ s	0.449 s	0.347 s	0.643 s
Level 2	$\tau_r \leq 3.0$ s	—	—	—
Level 3	$\tau_r \leq 10$ s	—	—	—

Careful consideration needs to be given to dynamic stability when performing design tradeoff studies, particularly those involving mass distribution and aerodynamic control surface sizing. The nonlinear simulation uncovered key aspects on tradeoff studies between longitudinal and lateral-directional stability modes through the PEGASUS iteration process. For longitudinal stability, increasing the horizontal tail area or adding a pitch damper can provide a higher pitch damping for PEGASUS 2.0 at the expense of an increase in vehicle weight, drag, and system complexity. For lateral-directional stability, a tradeoff between Dutch roll and spiral modes must be made when sizing the vertical tail. Having a large vertical tail provides good yaw damping and is required during a CLoT with PEGASUS's configuration. However, the large vertical tail size leads to an unstable spiral mode, though still with Level 1 flying qualities.

C. Limitations of the PEGASUS 2.0 Design

The results presented in this memorandum incorporated the latest design methodologies in an attempt to create a closed design. Examining the multi-views of PEGASUS 2.0 in Fig. 14, the vertical tail is large and the landing gear is long. Though these features are understandable due to the driving constraints, namely CLoT concerns with wingtip propulsors and maintaining a proper tipback angle, they highlight the risk of using an optimizer to size a vehicle without a complete set of constraints. A major challenge within aircraft design is that the number of design variables and constraints to completely define an aircraft geometry is large. As noted in the text, the vehicle was optimized to reduce CO_2e, but this analysis likely pushed the boundaries for the validity of the methods used.

The analysis did not consider the roll over angle for the aircraft in the multidisciplinary design optimization (MDO) environment, and this was reflected with a shallow roll-over angle. The landing gear would have to move away from the centerline to ensure the vehicle does not roll over during a sharp turn, and this movement spanwise would present challenges with respect to integrating the

landing gear within the fuselage or wing of the vehicle. A constraint on the roll-over angle would limit the cg location, likely moving it further aft, to keep the main landing gear length shorter. Of course, moving the cg location aft would also increase the size of the empennage, as an aft cg location shortens the moment arm between the empennage and the cg.

The vertical tail area is large compared to other aircraft of similar size due to the wingtip propulsors. The aerodynamic surrogates described in Section 3.2 revealed that the BLI propulsor did not provide a meaningful reduction in vehicle power consumption at cruise; however, the BLI propulsor would reduce the required thrust from the other propulsors through all phases of flight. The BLI propulsor's primary benefit may not come from decreasing the power at cruise so much as helping to reduce V_V. Because the BLI propulsor itself lies on the aircraft centerline, it does not generate an unbalanced moment with a CLoT, which is the main driver for V_V. Previous analysis [13] suggests that V_V is directly proportional to the wingtip propulsor thrust levels. Therefore, each one percent reduction in thrust at the wingtip should lead to a one percent reduction in V_V. Given this insight, the BLI propulsor may contribute a larger benefit than estimated in this research; though the benefit must be traded against the increased complexity (maintenance, weight/balance considerations, etc.) involved with the BLI propulsor's inclusion.

6. Concluding Remarks

The goal of this research was to integrate the various developments from past PEGASUS research into a cohesive, updated design called PEGASUS 2.0. The PEGASUS 2.0 sizing integrated PAI, structural considerations for wingtip propulsors, weight and balance constraints, and dynamic stability and flying qualities into a mission performance framework. Equivalent CO_2, or CO_2e, was used as the objective function for the vehicle-level sizing because of the challenges associated with using MTOW, fuel consumption, or energy consumption as objectives for hybrid-electric vehicles. PEGASUS 2.0 was compared against two reference vehicles, the advanced conventional baseline (ACB) and the hybrid-electric baseline (HEB). The ACB was created to prevent any disparities in technology level from obfuscating the benefits of the PEGASUS configuration over a traditional vehicle. The HEB was created to assess the benefits of the PEGASUS architecture, namely wingtip propulsors for cruise thrust with inboard motors for takeoff and climb assistance.

PAI CFD shows that the BLI propulsor originally planned for PEGASUS does not produce an appreciable benefit during cruise. Because of anticipated additional complexities with the addition of each propulsor, the BLI propulsor was removed from the PEGASUS 2.0 configuration. However, the calculated benefits of the BLI propulsor did not account for impacts on the vertical tail sizing. Using a BLI propulsor would have added thrust to the vehicle's centerline, reducing the thrust burden on the wing-borne propellers and, in turn, reducing the CLoT yawing moment that the vertical tail must overcome. The PAI surrogate model showed that the wingtip propellers yield a power reduction at cruise of approximately 11% compared to a conventional, inboard propulsion architecture.

This research shows that the PEGASUS 2.0 configuration is a heavier aircraft than the ACB and HEB. Much of the weight increase relative to the ACB is due to the battery required for the hybrid-electric propusion system, which is also reflected in the weight of the HEB. PEGASUS 2.0 has an additional weight increase due to the wingtip propulsors. The heavier MTOW of PEGASUS 2.0 necessitates a larger wing and more powerful propulsion system to maintain the same wing loading and thrust-to-weight ratio as the baselines. PEGASUS 2.0 needs a larger vertical tail than the two comparators due to the risk of losing a wingtip propulsor during the takeoff phase. Despite the size increases, PEGASUS 2.0 shows a reduction in fuel consumption and CO_2e relative to the

ACB and HEB. The HEB has 7.0% lower CO_2e emissions than the ACB, showing that hybridization can lead to reduced levels of CO_2e for an aircraft. PEGASUS 2.0 shows reductions in CO_2e of 12% and 18% relative to the HEB and ACB, respectively.

This study succeeded in introducing dynamic stability and flying qualities analysis into the conceptual design process to understand the implications of an advanced configuration such as PEGASUS. PEGASUS has Level 1 or 2 flying qualities for all longitudinal and lateral modes. Though the wingtip propulsors do not directly impact the flying qualities in a negative way, they contribute to large moments of inertias about the x- and z-axes that led to sluggish handling for roll subsidence. Further, the vertical tail size required to mitigate a CLoT at the wingtips causes PEGASUS 2.0 to have an unstable, but still Level 1, spiral mode, whereas the ACB and HEB have a stable spiral mode.

7. Future Work

The PEGASUS aircraft has had a rich set of analyses performed during its seven-year life. At this point, we plan to consider how design features and operational characteristics of the PEGASUS concept may translate to, and offer opportunities for, new concepts in the single-aisle and regional air mobility space that utilize EAP to reduce emissions, reduce noise, and improve performance in general. One area of this concept that remains unexplored is the use of wingtip propulsors primarily as control effectors. By reducing the required thrust at the wingtips, the CLoT challenges are mitigated, the inboard propulsors may be reduced in size, and control surface sizing and integration (ailerons and rudders) may be simplified. Though unexplored, these devices may also produce an induced drag reduction akin to thrust-producing wingtip propellers.

The PEGASUS research here and in the past highlighted the need for an integrated design environment for conceptual design. This research introduced more facets at higher fidelities than is commonly undertaken at the conceptual level. However, it is clear that we still failed to account for all the sizing constraints required. The landing gear placement is one example of a missed constraint. Though the tipback angle was implemented and maintained, the resulting tipover angle was violated and would require moving the landing gear off the fuselage. Another facet is certification constraints, Xie, et al. have shown the challenges that wingtip-mounted propellers pose for certification during a CLoT scenario using higher-fidelity tools than used within this memorandum [42, 43]. The authors advocate for stronger model-based systems engineering (MBSE) practices to incorporate MDO and have “a single source of truth” within a model. Further, MBSE promises to provide engineers the ability to look at a complete design in real time without overlooking key facets and requirements.

Appendix

A. Supplemental Contour Plots

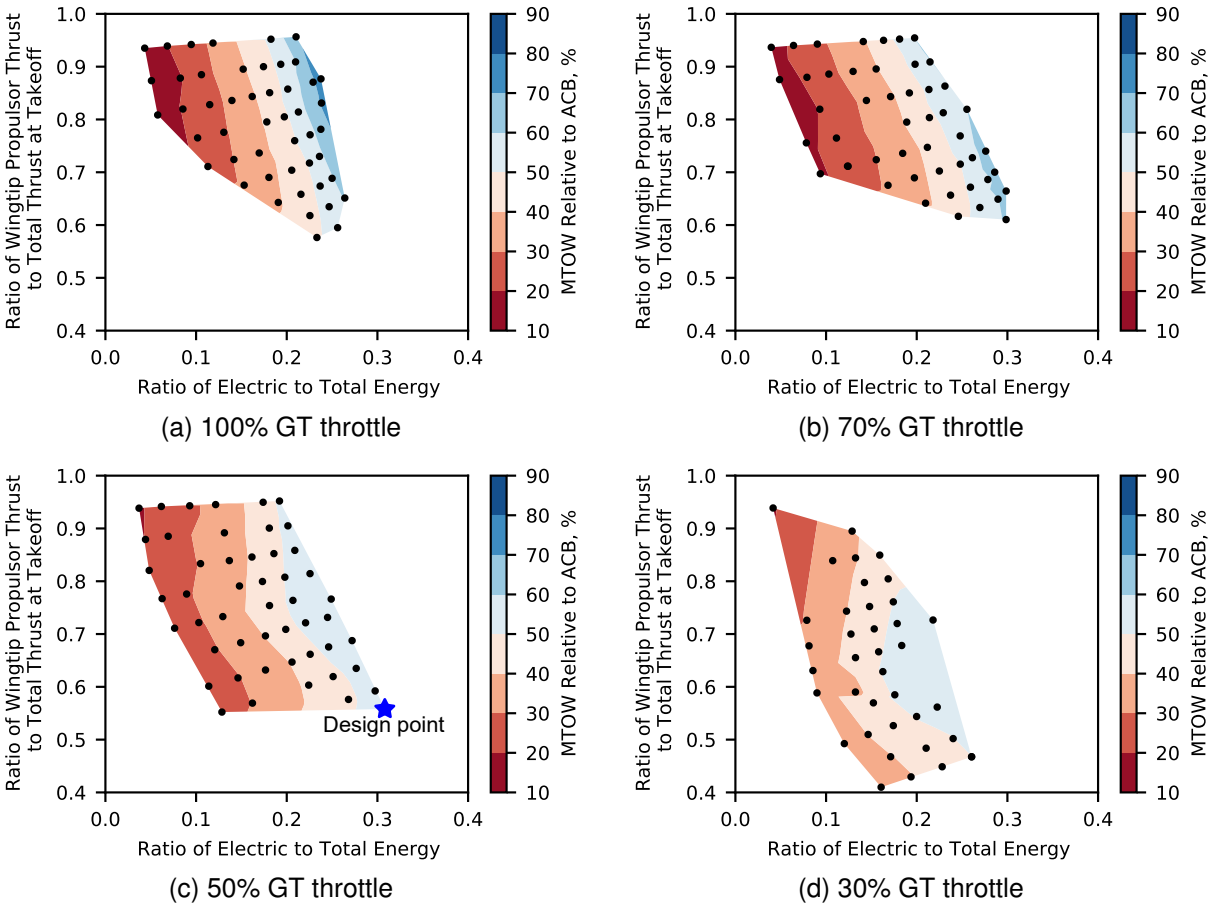

Figure A.1: Contours of percent change in maximum takeoff weight relative to the advanced conventional baseline for thrust split versus hybridization. The PEGASUS 2.0 configuration that minimizes CO_2e is shown with a blue star.

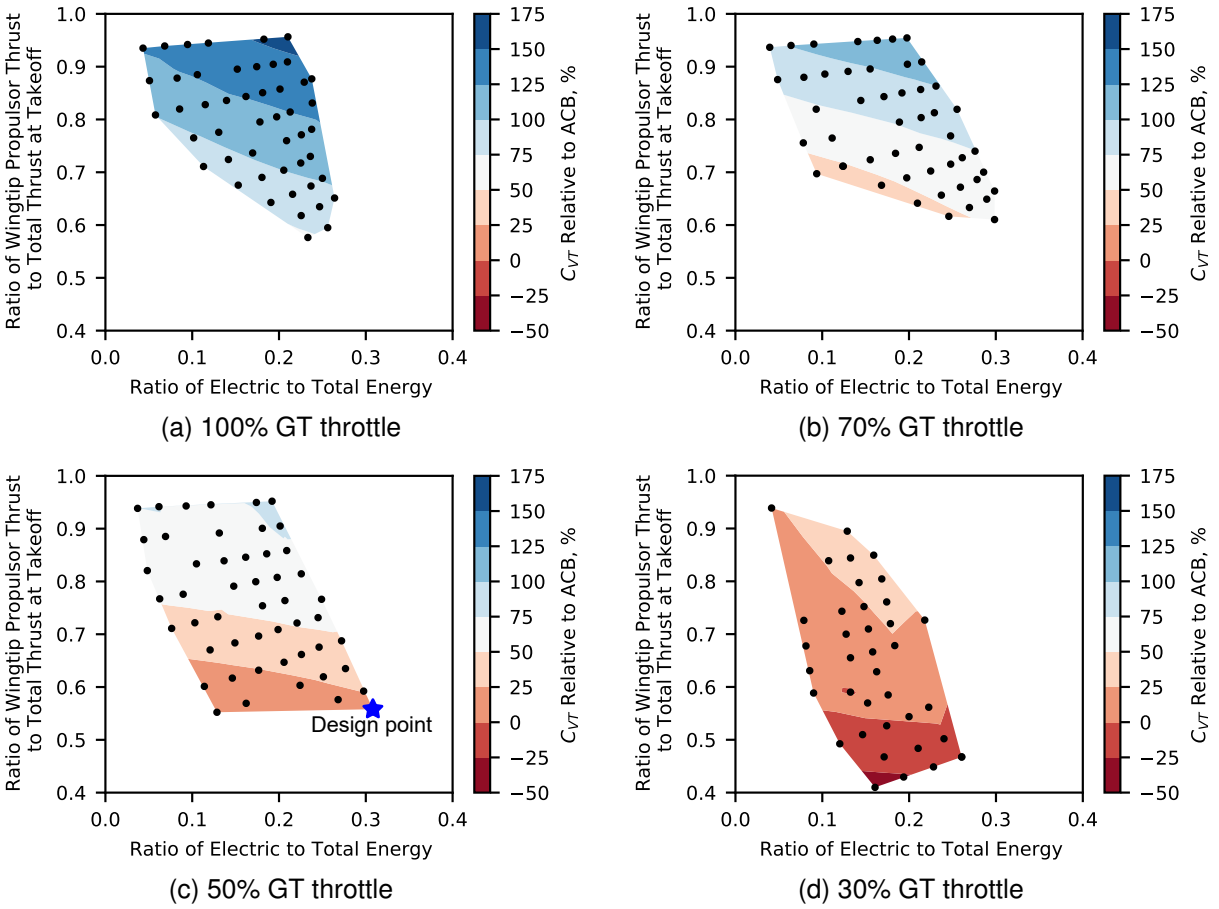

(a) 100% GT throttle

(b) 70% GT throttle

(c) 50% GT throttle

(d) 30% GT throttle

Figure A.2: Contours of percent change in vertical tail volume coefficient relative to the advanced conventional baseline for thrust split versus hybridization. The PEGASUS 2.0 configuration that minimizes CO_2e is shown with a blue star.

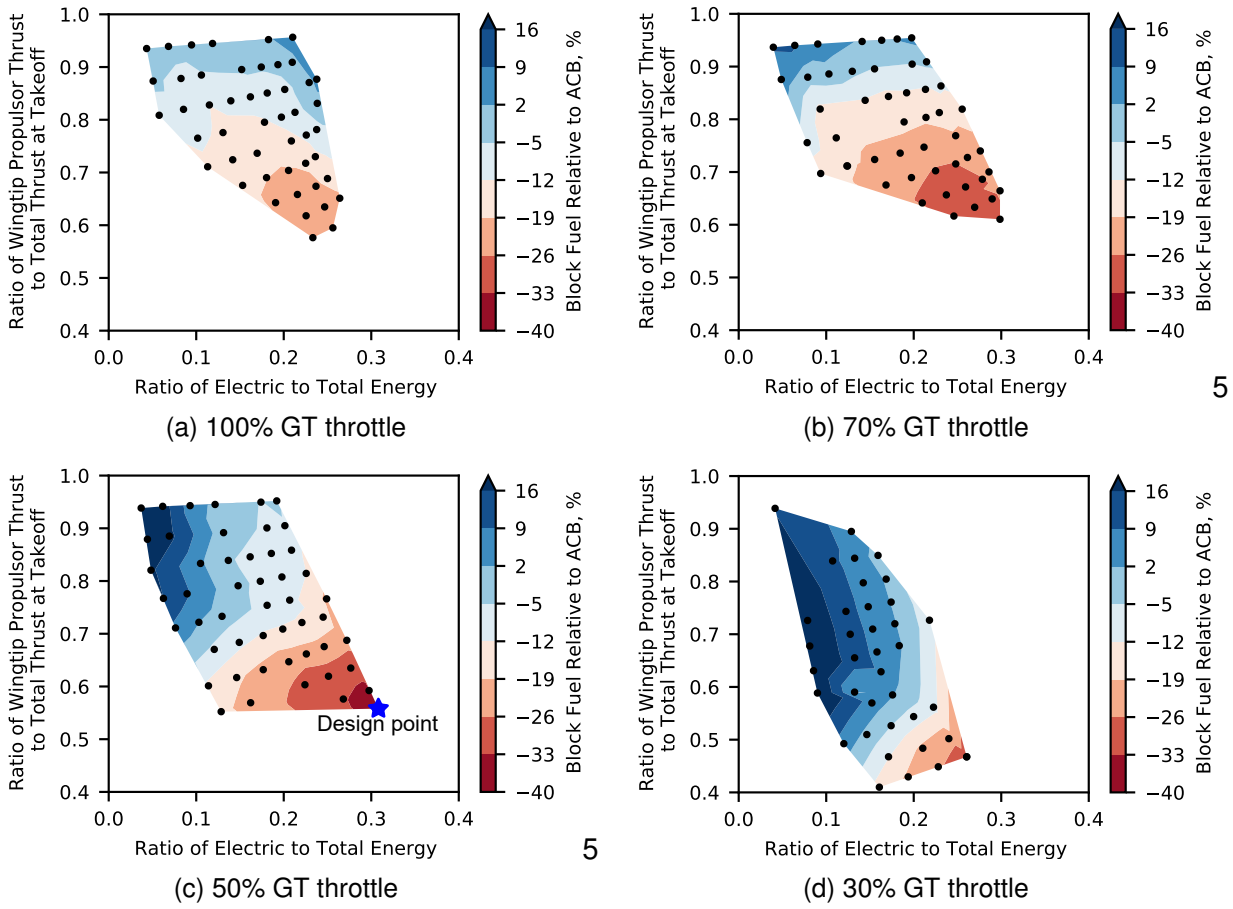

Figure A.3: Contours of percent change in block fuel relative to the advanced conventional baseline for thrust split versus hybridization. The PEGASUS 2.0 configuration that minimizes CO_2e is shown with a blue star.

References

[1] Antcliff, K. R., Guynn, M. D., Marien, T., Wells, D. P., Schneider, S. J., and Tong, M. J., "Mission Analysis and Aircraft Sizing of a Hybrid-Electric Regional Aircraft," No. 2016-1028 in AIAA SciTech Forum, American Institute of Aeronautics and Astronautics, 2016. doi: https://doi.org/10.2514/6.2016-1028.

[2] Antcliff, K. R., and Capristan, F. M., "Conceptual Design of the Parallel Electric-Gas Architecture with Synergistic Utilization Scheme (PEGASUS) Concept," No. 2017-4001 in AIAA AVIATION Forum, American Institute of Aeronautics and Astronautics, 2017. doi: https://doi.org/10.2514/6.2017-4001.

[3] Moore, M. D., and Goodrich, K. H., "High Speed Mobility through On-Demand Aviation," No. 2013-4373 in AIAA AVIATION Forum, American Institute of Aeronautics and Astronautics, 2013. doi: https://doi.org/10.2514/6.2013-4373.

[4] Moore, M. D., "Misconceptions of Electric Aircraft and their Emerging Aviation Markets," No. 2014-0535 in AIAA SciTech Forum, American Institute of Aeronautics and Astronautics, 2014. doi: https://doi.org/10.2514/6.2014-0535.

[5] Welstead, J., and Felder, J. L., "Conceptual Design of a Single-Aisle Turboelectric Commercial Transport with Fuselage Boundary Layer Ingestion," No. 2016-1027 in 54th AIAA Aerospace Sciences

Meeting, American Institute of Aeronautics and Astronautics, 2016. doi: https://doi.org/10.2514/6.2016-1027.

[6] Felder, J. L., Tong, M. T., Schnulo, S. L., Berton, J. J., Thacker, R. P., Haller, W. J., Kirk, J., and Guynn, M. D., "Updated Assessment of Turboelectric Boundary Layer Ingestion Propulsion Applied to Single-Aisle Commercial Transport," NASA Technical Memorandum, NASA TM-20210016661, NASA, Oct. 2022. URL https://ntrs.nasa.gov/citations/20210016661.

[7] Borer, N. K., Patterson, M. D., Viken, J. K., Moore, M. D., Bevirt, J., Stoll, A. M., and Gibson, A. R., "Design and Performance of the NASA SCEPTOR Distributed Electric Propulsion Flight Demonstrator," No. 2016-3920 in AIAA AVIATION Forum, American Institute of Aeronautics and Astronautics, 2016. doi: https://doi.org/10.2514/6.2016-3920.

[8] Blaesser, N. J., "Propeller-Wing Integration on the Parallel Electric-Gas Architecture with Synergistic Utilization Scheme (PEGASUS) Aircraft," No. 2019-1809 in AIAA SciTech Forum, American Institute of Aeronautics and Astronautics, 2019. doi: https://doi.org/10.2514/6.2019-1809.

[9] Capristan, F. M., and Blaesser, N. J., "Analysis of the Parallel Electric-Gas Architecture with Synergistic Utilization Scheme (PEGASUS) Concept," NASA Technical Memorandum, NASA TM-2019-220396, NASA, Aug. 2019. URL https://ntrs.nasa.gov/citations/20190030874.

[10] Capristan, F. M., and Welstead, J., "LEAPS: An Initial Assessment Towards a Multi-Order Approach to Air Vehicle Mission Analysis," No. 2017-4325 in AIAA AVIATION Forum, American Institute of Aeronautics and Astronautics, 2017. doi: https://doi.org/10.2514/6.2017-4325.

[11] Ordaz, I., Nielsen, E. J., and Wang, L., "Design of a Distributed Propulsion Concept Using an Adjoint-Based Approach and Blade Element Theory to Minimize Power," No. 2020-2632 in AIAA AVIATION Forum, American Institute of Aeronautics and Astronautics, 2020. doi: https://doi.org/10.2514/6.2020-2632.

[12] Biedron, R. T., Carlson, J.-R., Derlaga, J. M., Gnoffo, P. A., Hammond, D. P., Jacobson, K. E., Jones, W. T., Kleb, B., Lee-Rausch, E. M., Nielsen, E. J., Park, M. A., Rumsey, C. L., Thomas, J. L., Thompson, K. B., Walden, A. C., Wang, L., and Wood, W. A., "FUN3D Manual 13.7," NASA Technical Memorandum, NASA TM-2020-5010139, 2020. URL https://fun3d.larc.nasa.gov/papers/FUN3D_Manual-13.7_CORRECTED_COPY.pdf.

[13] Blaesser, N. J., and Frederick, Z. J., "Tail Sizing Considerations for Wingtip Propulsor Driven Aircraft Applied to the Parallel Electric-Gas Architecture with Synergistic Utilization Scheme (PEGASUS) Concept," No. 2020-2633 in AIAA AVIATION Forum, American Institute of Aeronautics and Astronautics, 2020. doi: https://doi.org/10.2514/6.2020-2633.

[14] Solano, D., Sarojini, D., Corman, J., and Mavris, D., "Parametric Structural Weight Estimation for the PEGASUS Concept Considering Dynamic Aeroelastic Effects," No. 2021-3086 in AIAA AVIATION Forum, American Institute of Aeronautics and Astronautics, 2021. doi: https://doi.org/10.2514/6.2021-3086.

[15] Frederick, Z. J., Blaesser, N. J., Valdez, F. D., and Hanson, C., "Weight and Balance Considerations for Electrified Aircraft Propulsion Applied to the Parallel Electric-Gas Architecture with Synergistic Utilization Scheme (PEGASUS) Concept," No. 2021-2449 in AIAA AVIATION Forum, American Institute of Aeronautics and Astronautics, 2021. doi: https://doi.org/10.2514/6.2021-2449.

[16] Wells, D. P., Horvath, B. L., and McCullers, L. A., "The Flight Optimization System Weights Estimation Method," NASA Technical Memorandum, NASA TM-2017-219627, NASA, 2017. URL https://ntrs.nasa.gov/citations/20170005851.

[17] McCullers, L. A., "Aircraft Configuration Optimization Including Optimized Flight Profiles," *Recent Experiences in Multidisciplinary Analysis and Optimization*, edited by J. Sobieski, NASA CP-2327, NASA, 1984, pp. 395–413. URL https://ntrs.nasa.gov/citations/19870002284.

[18] Gloudemans, J., Davis, P., and Gelhausen, P., "A Rapid Geometry Modeler for Conceptual Aircraft," No. 1996-0052 in Aerospace Sciences Meetings, American Institute of Aeronautics and Astronautics, 1996. doi: https://doi.org/10.2514/6.1996-52.

[19] Ordaz, I., Rallabhandi, S. K., and Nielsen, E. J., "Adjoint-Based Design of a Distributed Propulsion Concept with a Power Objective," No. 2019-3681 in AIAA AVIATION Forum, American Institute of Aeronautics and Astronautics, 2019. doi: https://doi.org/10.2514/6.2019-3681.

[20] "FUN3D Resource Website," Online, Accessed: December 2021. URL https://fun3d.larc.nasa.gov.

[21] "Scikit-Learn Website," Online, Accessed: December 2021. URL https://scikit-learn.org.

[22] "SciPy Website," Online, Accessed: December 2021. URL https://scipy.org.

[23] "Cadence Website," Online, Accessed: December 2021. URL https://www.pointwise.com.

[24] "Helden Aerospace Website," Online, Accessed: December 2021. URL https://heldenaero.com/heldenmesh.

[25] Gill, P. E., Murray, W., and Saunders, M. A., "SNOPT: An SQP Algorithm for Large-Scale Constrained Optimization," *SIAM Review*, Vol. 47, No. 1, 2005, pp. 99–131.

[26] Gray, J. S., Kenway, G. K., Mader, C. A., and Martins, J., "Aero-propulsive Design Optimization of a Turboelectric Boundary Layer Ingestion Propulsion System," No. 2016-3976 in AIAA AVIATION Forum, American Institute of Aeronautics and Astronautics, 2018. doi: https://doi.org/10.2514/6.2018-3976.

[27] Lytle, J. K., "The Numerical Propulsion System Simulation: An Overview," NASA Technical Memorandum, NASA TM-2000-209915, NASA, 2000. URL https://ntrs.nasa.gov/citations/20000063377.

[28] Drela, M., and Youngren, H., "XROTOR Download Page," Online, Mar. 2011. URL http://web.mit.edu/drela/Public/web/xrotor/, accessed Nov. 2018.

[29] Marien, T., Blaesser, N. J., Guynn, M. D., Kirk, J., Frederick, Z. J., Fisher, K., Schnieder, S., Thacker, R., and Frederic, P., "Methodology Used for an Electrified Aircraft Propulsion Design Exploration," No. 2021-3191 in AIAA AVIATION Forum, American Institute of Aeronautics and Astronautics, 2021. doi: https://doi.org/10.2514/6.2021-3191.

[30] Marien, T., Blaesser, N. J., Guynn, M. D., Kirk, J., Frederick, Z. J., Fisher, K., Schnieder, S., Thacker, R., and Frederic, P., "Results for an Electrified Aircraft Propulsion Design Exploration," No. 2021-3280 in AIAA Propulsion and Energy 2021 Forum, American Institute of Aeronautics and Astronautics, 2021. doi: https://doi.org/10.2514/6.2021-3280.

[31] Caughey, D. A., "Introduction to Aircraft Stability and Control Course Notes for M&AE 5070," Online, June 2011. URL https://courses.cit.cornell.edu/mae5070/Caughey_2011_04.pdf.

[32] "Simulation and Model-Based Design," Online, Accessed: May 2020. URL https://www.mathworks.com/products/simulink.html.

[33] Department of Defense, "Flying Qualities of Piloted Aircraft," MIL Standard, MIL-STD-1797, DoD, 2006.

[34] Department of Defense, "Military Specification Flying Qualities of Piloted Airplanes," MIL Standard, MIL-F-8785, DoD, 1980.

[35] Powers, B. G., "Analytical Study of Ride Smoothing Benefits of Control System Configurations Optimized for Pilot Handling Qualities," NASA Technical Paper, NASA TP-1148, NASA, 1978. URL https://ntrs.nasa.gov/citations/19780010133.

[36] FSF Editorial Staff, "Boeing 737 Postmaintenance Test Flight Encounters Uncommanded Roll-and-yaw Oscillations," *Flight Safety Foundation*, Vol. 55, No. 5, 1998, pp. 1–8.

[37] Federal Aviation Administration, *Airplane Flying Handbook*, FAA-H-8083-3C, Department of Transportation, 2021, Chap. 13: Transition to Multiengine Airplanes.

[38] Talay, T. A., "Introduction to the Aerodynamics of Flight," NASA Special Publication, NASA SP-367, NASA, 1975.

[39] Federal Aviation Administration, *Flight Training Handbook*, AC 61-21A, Department of Transportation, 1965, Chap. 17: Principles of Flight and Performance Characteristics.

[40] Hunsaker, J. C., "Dynamical Stability of Aeroplanes," *Proceedings of the National Academy of Sciences*, Vol. 2, No. 5, 1916, pp. 278–288.

[41] Szalai, K. J., "The Influence of Response Feedback Loops on the Lateral-Directional Dynamics of a Variable-Stability Transport Aircraft," NASA Technical Note, NASA TN D-3966, NASA, 1967. URL https://ntrs.nasa.gov/citations/19670017216.

[42] Xie, J., Cai, Y., Sarojini, D., Harrison, E. D., and Mavris, D. N., "Certification-Constrained Vertical Tail Sizing and Power Split Optimization for Distributed Electric Propulsion Aircraft," *Journal of Aircraft*, Vol. 60, No. 4, 2023, pp. 1272–1289. doi: https://doi.org/10.2514/1.C037239.

[43] Xie, J., Harrison, E., and Mavris, D. N., "Quantifying Impacts of Uncertainties on Certification-Driven Design," No. 2023-4194 in AIAA AVIATION, American Institute of Aeronautics and Astronautics, 2023. doi: https://doi.org/10.2514/6.2023-4194.